INRIA

INSTITUT NATIONAL DE RECHERCHE EN INFORMATIQUE ET EN AUTOMATIQUE

Identification of generalized impedance boundary conditions: some numerical issues

Laurent Bourgeois — Nicolas Chaulet — Houssem Haddar

N° 7449

November 2010

Thème NUM

ISSN 0249-6399 ISRN INRIA/RR--7449--FR+ENG

INSTITUT NATIONAL
DE RECHERCHE
EN INFORMATIQUE
ET EN AUTOMATIQUE

INRIA

centre de recherche
SACLAY - ÎLE-DE-FRANCE

Identification of generalized impedance boundary conditions: some numerical issues

Laurent Bourgeois* , Nicolas Chaulet† , Houssem Haddar†

Thème NUM — Systèmes numériques
Équipe-Projet DeFI

Rapport de recherche n° 7449 — November 2010 — 30 pages

Abstract: We are interested in the identification of a Generalized Impedance Boundary Condition from the far fields created by one or several incident plane waves at a fixed frequency. We focus on the particular case where this boundary condition is expressed as a second order surface operator: the inverse problem then amounts to retrieve the two functions λ and μ that define this boundary operator. We first derive a new type of stability estimate for the identification of λ and μ from the far field when inexact knowledge of the boundary is assumed. We then introduce an optimization method to identify λ and μ, using in particular a H^1-type regularization of the gradient. We lastly show some numerical results in two dimensions, including a study of the impact of some various parameters, and by assuming either an exact knowledge of the shape of the obstacle or an approximate one.

Key-words: Inverse scattering, Generalized Impedance Boundary Condition, Stability estimate, Steepest descent method

* Laboratoire POEMS, ENSTA, 32, Boulevard Victor, 75739 Paris Cedex 15, France
† INRIA Saclay Ile de France / CMAP Ecole Polytechnique, Route de Saclay, 91128 Palaiseau Cedex FRANCE

Centre de recherche INRIA Saclay – Île-de-France
Parc Orsay Université
4, rue Jacques Monod, 91893 ORSAY Cedex
Téléphone : +33 1 72 92 59 00

Identification de conditions d'impédances généralisées: quelques aspects numériques

Résumé : Ce travail concerne l'identification d'une condition aux limites d'impédance généralisée (GIBC) sur le bord d'un objet diffractant à partir du champ lointain créé par une ou plusieurs ondes planes, dans le cas particulier où cette condition est caractérisée par un opérateur d'ordre 2 sur le bord, défini par deux fonctions λ et μ à identifier. Nous commençons par établir une estimation originale de stabilité des fonctions λ et μ cherchées vis à vis du champ lointain, en présence d'une erreur commise sur la forme de l'obstacle. Nous introduisons ensuite une méthode d'optimisation pour identifier λ et μ, une régularisation de type H^1 du gradient étant utilisée. Nous montrons enfin des résultats numériques de reconstruction en deux dimensions incluant une étude de sensibilité par rapport aux différents paramètres, en supposant une connaissance exacte ou approchée de la forme de l'obstacle.

Mots-clés : Diffraction inverse, Condition d'impédance généralisée, Estimation de stabilité, Méthode de gradient

1 Introduction

We are interested in this work by the identification of boundary coefficients in so–called Generalized Impedance Boundary Conditions (GIBC) on a given obstacle from measurements of the scattered field far from the obstacle associated with one or several incident plane waves at a given frequency. More specifically we shall consider boundary conditions of the type

$$\frac{\partial u}{\partial \nu} + \mathrm{div}_{\partial D}(\mu \nabla_{\partial D} u) + \lambda u = 0 \quad \text{ on } \partial D$$

where μ and λ are complex valued functions, $\mathrm{div}_{\partial D}$ and $\nabla_{\partial D}$ are respectively the surface divergence and the surface gradient on ∂D and ν denotes the outward unit normal on ∂D. In the case $\mu = 0$ this condition is the classical impedance boundary condition (also known as the Leontovitch boundary condition) used for instance to model imperfectly conducting obstacles. The wider class of GIBCs is commonly used to model thin coatings or gratings as well as more accurate models for imperfectly conducting obstacles (see [2, 8, 9, 10]). Addressing this problem is motivated by applications in non destructive testing, identification problems or modeling related to stealth technology or antennas. The use of GIBCs has at least two advantages for the inverse problem as compared to the use of an exact model. First, the identification problem becomes less unstable. Second, since solving the forward problem with GIBC is less time consuming, using such model in iterative non–linear methods is more advantageous.

The classical case $\mu = 0$ has been addressed in the literature by several authors, from the mathematical point of view in [18, 14] and from the numerical point of view in [5, 6]. The problem of recovering both the shape of the obstacle and the impedance coefficient is also considered in [15, 17, 19, 20]. The case of GIBC has only been recently addressed in [3] where uniqueness and local stability results have been reported.

The present work complements these first investigations in two directions. The first one is on the theoretical level. We prove stability of the reconstruction of the impedances on a perturbed geometry relying on two properties:

- continuity of the far field with respect to the obstacle, uniformly with respect to the impedance coefficients,
- stability for the inverse coefficient problem for a known obstacle.

This kind of stability result would be useful for instance when the geometry has been itself reconstructed from measurements using some qualitative methods (e.g. sampling methods [4, 12]) and therefore is known only approximately. This result may be also useful in understanding the convergence of iterative methods to reconstruct both the obstacle and the coefficients where the updates for the geometry and the physical parameters are made alternatively. Let us also mention that the proof of our stability result can be straightforwardly extended to other identification problems that enjoy the two properties indicated above.

In a second part, we investigate a numerical optimization method to identify the boundary coefficients. We propose a reconstruction procedure based on a steepest descent method with $H^1(\partial D)$ regularization of the gradient. The accuracy and stability of the inversion scheme is tested through various numerical

experiments in a $2D$ setting. Special attention is given to the case of non regular coefficients and inexact knowledge of the boundary ∂D.

The outline of our article is the following. In section 2 we introduce and study the forward and inverse problems. Section 3 is dedicated to the derivation of a stability result with respect to the geometry. The numerical part is the subject of section 4.

2 The forward and inverse problem

2.1 The forward scattering problem

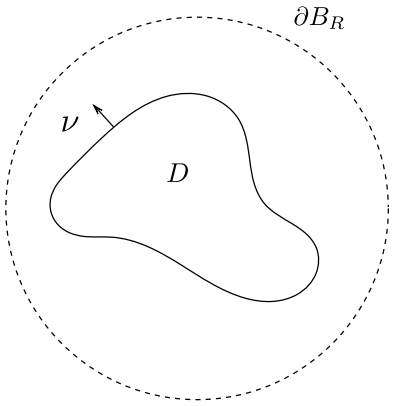

Figure 1: *Configuration of the problem.*

Let D be an open bounded domain of $\mathbb{R}^d$, $d = 2$ or 3 with a Lipschitz continuous boundary ∂D, $\Omega = \mathbb{R}^d \setminus \overline{D}$ and $(\lambda, \mu) \in L^\infty(\partial D)^2$ the impedance coefficients. The scattering problem with generalized impedance boundary conditions (GIBC) consists in finding $u = u^s + u^i$ such that

$$\begin{cases} \Delta u + k^2 u = 0 \quad \text{in } \Omega \\ \text{div}_{\partial D}(\mu \nabla_{\partial D} u) + \dfrac{\partial u}{\partial \nu} + \lambda u = 0 \quad \text{on } \partial D \end{cases} \tag{1}$$

and u^s satisfies the Sömmerfeld radiation condition

$$\lim_{R \to \infty} \int_{|x|=R} \left| \frac{\partial u^s}{\partial r} - iku^s \right|^2 ds = 0$$

where

- k is the wave number,
- $u^i = e^{ik\hat{d}\cdot x}$ is an incident plane wave where $\hat{d}$ belongs to the unit sphere of $\mathbb{R}^d$ denoted S^{d-1},
- $u^s \in V := \{v \in \mathcal{D}'(\Omega), \varphi v \in H^1(\Omega) \, \forall \, \varphi \in \mathcal{D}(\mathbb{R}^d) \text{ and } v_{|\partial D} \in H^1(\partial D)\}$ is the scattered field,

- $\mathrm{div}_{\partial D}$ and $\nabla_{\partial D}$ are respectively the surface divergence and the surface gradient on ∂D,
- ν is the outward unit normal on ∂D.

For a precise definition of the surface operators we refer to Chapter 5 of [11]. For $v \in H^1(\partial D)$ the surface gradient $\nabla_{\partial D} v$ lies in $L^2_t(\partial D) := \{V \in (L^2(\partial D))^d\,,\, V \cdot \nu = 0\}$. Moreover, $\mathrm{div}_{\partial D}(\mu \nabla_{\partial D} u)$ is defined in $H^{-1}(\partial D)$ for $\mu \in L^\infty(\partial D)$ by

$$\langle \mathrm{div}_{\partial D}(\mu \nabla_{\partial D} u), v \rangle_{H^{-1}(\partial D), H^1(\partial D)} := -\int_{\partial D} \mu \nabla_{\partial D} u \cdot \nabla_{\partial D} v ds \quad \forall v \in H^1(\partial D)\,.$$

In order to prove well–posedness of the solution of problem (1) and then to numerically solve the problem, we introduce the so–called Dirichlet–to–Neumann map so that we can can give an equivalent formulation of (1) in a bounded domain $\Omega_R = \Omega \cap B_R$ where B_R is the ball of radius R such that $D \subset B_R$. The Dirichlet–to–Neumann map, $S_R : H^{1/2}(\partial B_R) \mapsto H^{-1/2}(\partial B_R)$ is defined for $g \in H^{1/2}(\partial B_R)$ by $S_R g := \partial u^e / \partial r|_{\partial B_R}$ where u^e is the radiating solution of the Helmholtz equation outside B_R and $u^e = g$ on ∂B_R. We have the following properties (see [16] p.97)

$$\Re e \langle S_R g, g \rangle \leq 0 \;\text{ and }\; \Im m \langle S_R g, g \rangle \geq 0 \quad \forall g \in H^{1/2}(\partial B_R),$$

where $\langle \cdot, \cdot \rangle$ is the duality product between $H^{-1/2}(\partial B_R)$ and $H^{1/2}(\partial B_R)$. Solving (1) is equivalent to find u in $V_R := \{v \in H^1(\Omega_R);\, v_{|\partial D} \in H^1(\partial D)\}$ such that:

$$\mathcal{P}(\lambda, \mu, \partial D) \qquad \begin{cases} \Delta u + k^2 u = 0 \quad \text{inside } \Omega_R \\ \mathrm{div}_{\partial D}(\mu \nabla_{\partial D} u) + \dfrac{\partial u}{\partial \nu} + \lambda u = 0 \quad \text{on } \partial D \\ \dfrac{\partial u}{\partial r} - S_R(u) = \dfrac{\partial u^i}{\partial r} - S_R(u^i) \;\text{ on } \partial B_R \end{cases} \tag{2}$$

We assume

Assumption ($\mathcal{H}1$)

- ∂D is Lipschitz continuous,
- $(\lambda, \mu) \in (L^\infty(\partial D))^2$ are such that

$$\Im m(\lambda) \geq 0\,,\; \Im m(\mu) \leq 0 \quad \text{a.e. in } \partial D$$

and there exists $c > 0$ such that

$$\Re e(\mu) \geq c \qquad \text{a.e. in } \partial D.$$

In the following, K will be a compact subset of $(L^\infty(\partial D))^2$ such that there exists a constant $c_K > 0$ such that if $(\lambda, \mu) \in K$ then assumption ($\mathcal{H}1$) holds with the constant $c = c_K$.

Theorem 2.1. *If assumption ($\mathcal{H}1$) is satisfied then problem $\mathcal{P}(\lambda, \mu, \partial D)$ has a unique solution u in V_R.*

Proof. In order to prove this result, we use the variational formulation of (2) given by : find $u \in V_R$ such that for all $v \in V_R$

$$a(u,v) = l(v)\,,$$

with

$$a(u,v) := \int_{\Omega_R} (\nabla u \cdot \nabla \overline{v} - k^2 u\overline{v})dx + \int_{\partial D} (\mu \nabla_{\partial D} u \cdot \nabla_{\partial D}\overline{v} - \lambda u\overline{v})ds - \langle S_R u, v\rangle$$

$$l(v) := \int_{\partial B_R} \left(\frac{\partial u^i}{\partial r} - S_R(u^i)\right)\overline{v}ds$$

Remark that V_R equipped with the scalar product $(\cdot,\cdot)_{V_R} := (\cdot,\cdot)_{H^1(\Omega_R)} + (\cdot,\cdot)_{H^1(\partial D)}$ is a Hilbert space. Thanks to the Riesz representation theorem we define two operators J_R and K_R from V_R into itself that satisfy for all $u,\ v\ \in V_R$

$$(J_R u, v)_{V_R} = (u,v)_{H^1(\Omega_R)} + \int_{\partial D} (\mu \nabla_{\partial D} u \cdot \nabla_{\partial D}\overline{v})ds - \langle S_R u, v\rangle,$$

$$(K_R u, v)_{V_R} = -(1+k^2)(u,v)_{L^2(\Omega_R)} - \int_{\partial D} \lambda u\overline{v}ds$$

and F_R an element of V_R uniquely determined by

$$(F_R, v)_{V_R} = l(v) \qquad \forall v \in V_R.$$

The variational formulation is equivalent to find $u \in V_R$ such that

$$(J_R + K_R)u = F_R \quad \text{in } V_R\,.$$

As soon as $\Re e(\mu(x)) \geq c > 0$ for almost every $x \in \partial D$ the operator J_R is an isomorphism of V_R. Moreover the Rellich theorem tells us that $H^1(\Omega_R)$ and $H^1(\partial D)$ are compactly embedded into $L^2(\Omega_R)$ and $L^2(\partial D)$ respectively. From that we deduce that K_R is a compact operator on V_R and therefore our problem is of Fredholm type. As a consequence, it is sufficient to prove uniqueness to have existence. Let u be satisfying

$$a(u,v) = 0 \qquad \forall v \in V_R$$

then taking $v = u$ and the imaginary part of this equation we have

$$\int_{\partial D} (\Im m(\mu)|\nabla_{\partial D} u|^2 - \Im m(\lambda)|u|^2)ds - \Im m\langle S_R u, u\rangle = 0.$$

Assumption ($\mathcal{H}1$) implies that

$$\Im m\langle S_R u, u\rangle = 0$$

which implies that $u|_{\partial B_R} = 0$ (see [16] p. 103). Therefore $\frac{\partial u}{\partial r}|_{\partial B_R} = S_R u = 0$ thanks to the boundary condition on ∂B_R. To conclude, u is solution to a Cauchy problem inside Ω_R with data equal to zero on ∂B_R, hence $u = 0$ on Ω_R and $\mathcal{P}(\lambda, \mu, \partial D)$ has a unique solution in V_R. □

For λ and μ satisfying $(\mathcal{H}1)$ let us define the operator $A_{\lambda,\mu}$ by

$$(A_{\lambda,\mu}u, v)_{V_R} = \int_{\Omega_R} (\nabla u \cdot \nabla \overline{v} - k^2 u\overline{v}) dx + \int_{\partial D} (\mu \nabla_{\partial D} u \cdot \nabla_{\partial D} \overline{v} - \lambda u \overline{v}) ds - \langle S_R u, v \rangle.$$

The map

$$(\lambda, \mu) \longmapsto A_{\lambda,\mu} \in \mathcal{L}(V_R, V_R)$$

where $\mathcal{L}(V_R, V_R)$ is the set of bounded operators on V_R, is continuous and for every (λ, μ) that satisfy $(\mathcal{H}1)$ $A_{\lambda,\mu}$ is invertible on V_R. We establish in the following an uniform bound for its inverse $A^{-1}_{\lambda,\mu}$ with respect to the impedance coefficients.

Proposition 2.2. *There exists a constant $C_K > 0$ such that for every $(\lambda, \mu) \in K$*

$$|||A^{-1}_{\lambda,\mu}||| \leq C_K$$

where $|||\cdot|||$ stands for operators norm.

Proof. Consider the map

$$\mathcal{A} : \quad (\lambda, \mu) \in K \longmapsto A^{-1}_{\lambda,\mu} \in \mathcal{L}(V_R, V_R).$$

We shall prove that this map is continuous and since K is compact, we obtain the desired uniform estimate. Take $(\lambda, \mu) \in K$ and $(h, l) \in (L^\infty(\partial D))^2$ such that $(\lambda + h, \mu + l) \in K$ and for $F \in V_R$ define u and $u_{h,l}$ in V_R by

$$A_{\lambda,\mu} u = F$$

$$A_{\lambda+h,\mu+l} u_{h,l} = F.$$

We have

$$\|A^{-1}_{\lambda+h,\mu+l} F - A^{-1}_{\lambda,\mu} F\|_{V_R} = \|u_{h,l} - u\|_{V_R} = \|A^{-1}_{\lambda+h,\mu+l}(A_{\lambda,\mu} - A_{\lambda+h,\mu+l})u\|_{V_R}$$

but $A_{\lambda,\mu}$ depends continuously on (λ, μ)

$$\lim_{(h,l)\to 0} |||A_{\lambda,\mu} - A_{\lambda+h,\mu+l}||| = 0 \tag{3}$$

and using the results on Neumann series of chapter 10 in [13] there exists a constant $C(\lambda, \mu)$ which depends on λ and μ such that for every (h, l) sufficiently small

$$|||A^{-1}_{\lambda+h,\mu+l}||| \leq C(\lambda, \mu). \tag{4}$$

(3) and (4) together imply that

$$\lim_{(h,l)\to 0} |||A^{-1}_{\lambda+h,\mu+l} - A^{-1}_{\lambda,\mu}||| = 0$$

in other words, the map $\mathcal{A}$ is continuous on the compact set K. □

From now on we shall denote $A := A_{\lambda,\mu}$. Under the sufficient conditions $(\mathcal{H}1)$ on the impedance coefficients λ and μ that ensure existence and uniqueness for the forward problem we can study the inverse coefficients problem and this is the aim of the next section.

2.2 Formulation of the inverse problem

We recall the following asymptotic behaviour for the scattered field (see [7]):

$$u^s(x) \sim \frac{e^{ikr}}{r^{(d-1)/2}} \left(u^\infty(\hat{x}) + O\left(\frac{1}{r}\right)\right) \qquad r \longrightarrow +\infty$$

uniformly for all the directions $\hat{x} = x/r \in S^{d-1}$. The far–field $u^\infty \in L^2(S^{d-1})$ is uniquely determined by this expression and we have an integral representation on the boundary Γ of some regular open domain that contains D :

$$u^\infty(\hat{x}) = \int_\Gamma \left(u^s(y) \frac{\partial \Phi^\infty(y,\hat{x})}{\partial \nu(y)} - \frac{\partial u^s(y)}{\partial \nu} \Phi^\infty(y,\hat{x}) \right) ds(y) \quad \forall \hat{x} \in S^{d-1}, \qquad (5)$$

where Φ^∞ is the far–field associated with the Green function of the Helmholtz equation and is defined by

$$\begin{aligned} \text{in } \mathbb{R}^2 \qquad \Phi^\infty : \quad & (y,\hat{x}) \in \mathbb{R}^2 \times S^1 \longmapsto \frac{e^{i\pi/4}}{\sqrt{8\pi k}} e^{-iky\cdot\hat{x}} \\ \text{in } \mathbb{R}^3 \qquad \Phi^\infty : \quad & (y,\hat{x}) \in \mathbb{R}^3 \times S^2 \longmapsto \frac{1}{4\pi} e^{-iky\cdot\hat{x}}, \end{aligned}$$

and the second integral has to be understood as a duality product between $H^{-1/2}(\Gamma)$ and $H^{1/2}(\Gamma)$. We can also define the far–field map

$$T : \quad (\lambda, \mu, \partial D) \to u^\infty$$

where u^∞ is the far–field associated with the scattered field $u^s = u - u^i$ and u is the unique solution of problem $\mathcal{P}(\lambda, \mu, \partial D)$. The inverse coefficients problem is the following : given

- an obstacle D
- an incident direction $d \in S^{d-1}$,
- its associated far–field pattern u^∞ for all $\hat{x} \in S^{d-1}$,

reconstruct the corresponding impedance coefficients λ and μ. In other words the inverse problem amounts to invert the map T with respect to the coefficients λ and μ for a given ∂D. The first natural question related to this inverse problem is injectivity of T and stability properties of the inverse map. These questions have been addressed in [3] where for instance results on local stability in compact sets have been reported. Our subsequent analysis on the stability with respect to perturbed obstacles of the reconstruction of λ and μ will depend on stability for the inverse map of T. We therefore shall assume the following

Assumption ($\mathcal{H}2$)

- there exists a compact $K \subset (L^\infty(\partial D))^2$ such that for $(\lambda, \mu) \in K$ there exists a constant $C(\lambda, \mu, K)$ which depends on λ, μ and K such that for every $(\widetilde{\lambda}, \widetilde{\mu}) \in K$ we have

$$\begin{aligned} \|\lambda - \widetilde{\lambda}\|_{L^\infty(\partial D)} + & \|\mu - \widetilde{\mu}\|_{L^\infty(\partial D)} \\ & \leq C(\lambda, \mu, K) \|T(\lambda, \mu, \partial D) - T(\widetilde{\lambda}, \widetilde{\mu}, \partial D)\|_{L^2(S^d)} . \end{aligned}$$

We refer to [3] for examples of compacts K for which $(\mathcal{H}2)$ holds. We notice for instance that uniqueness with single incident wave fails in general except if one assumes that parts of λ and μ are known *a priori*. Moreover we may need to add some restriction for the incident direction or for the geometry of the obstacle (see [3] for more details). There are also global stability results available in the literature (that is $C(\lambda, \mu, K)$ does not depend on λ) for classical impedance boundary conditions (i.e. $\mu = 0$), see [14, 18].

Remark 2.3. *u^∞ is an analytical function on S^{d-1} (see [7]) hence assuming that we know the far–field everywhere on S^{d-1} is equivalent to assume that we know it on a non–empty part of S^{d-1}.*

3 A stability estimate for the impedances in the presence of a perturbed obstacle

3.1 The forward and inverse problems on a perturbed obstacle

The question we will try to answer in this section concerns the stability of the reconstruction of the impedances with respect to the geometry ∂D : assume that we reconstruct the impedance coefficients on a "perturbed" obstacle, do we have some stability estimates on this reconstruction?

Remark 3.1. *Here "perturbed" means that we have an approximate knowledge of the obstacle (see Figure 2) that can be obtained after (or during) a numerical reconstruction of the obstacle for example. More precisely, we may need the stability result we present hereafter to ensure convergence of hybrid reconstruction methods of both the impedance coefficients and the obstacle as presented in [5], [19] or [17] for the case of a classical impedance condition.*

First we shall define the "perturbed" problem and then present a continuity result with respect to the obstacle uniformly with respect to the impedance coefficients. The stability result is then deduced thanks to the stability estimate for the inverse coefficients problem with a known obstacle given in assumption $(\mathcal{H}2)$.

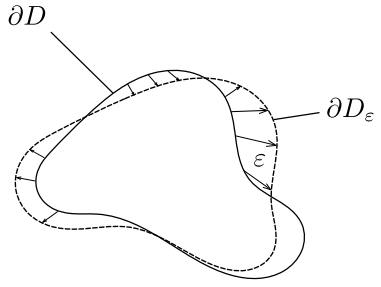

Figure 2: *Illustration of the "perturbed" geometry.*

We assume that D is of class C^1 and we consider problem (2) with a "perturbed" geometry $D_\varepsilon \subset B_R$ of D. We say that D_ε is a perturbation of D as soon as

one can find a function $\varepsilon \in (C^1(\mathbb{R}^d))^d$ sufficiently small so that $Id + \varepsilon$ is a C^1–diffeomorphism and

$$\partial D_\varepsilon = \{x + \varepsilon(x)\ ;\ x \in \partial D\}\,.$$

Recall that whenever $\|\varepsilon\|_{(W^{1,\infty}(\mathbb{R}^d))^d} < 1$ the map $f_\varepsilon := Id + \varepsilon$ where Id stands for the identity of $\mathbb{R}^d$, is a C^1–diffeomorphism of $\mathbb{R}^d$ (see chap 5. of [11]).

The inverse problem. In this situation of perturbed knowledge of the obstacle, the inverse problem consists in finding the better approximations λ_ε and μ_ε of the exact impedance coefficients for example minimizing the distance between $T(\lambda, \mu, \partial D)$ and the far–field $T(\lambda_\varepsilon, \mu_\varepsilon, \partial D_\varepsilon)$. Following this idea, let us assume that for some $\delta \geq 0$

$$\|T(\lambda_\varepsilon, \mu_\varepsilon, \partial D_\varepsilon) - T(\lambda, \mu, \partial D)\|_{L^2(S^{d-1})} \leq \delta\,.$$

From this information and from the distance between ∂D and ∂D_ε, can we have an estimate on the boundary coefficients? In other words, do we have

$$\|\lambda_\varepsilon \circ f_\varepsilon - \lambda\|_{L^\infty(\partial D)} + \|\mu_\varepsilon \circ f_\varepsilon - \mu\|_{L^\infty(\partial D)} \leq g(\delta, \varepsilon) \tag{6}$$

for some function g such that $g(\delta, \varepsilon) \to 0$ as $\delta \to 0$ and $\varepsilon \to 0$? In order to prove such a result, we first need a continuity property of T with respect to ∂D.

3.2 Continuity of the far–field with respect to the obstacle

In the following, for a given $\varepsilon_0 > 0$ we assume that

Assumption ($\mathcal{H}3$)

- D is an open bounded domain of $\mathbb{R}^d$ of class C^1,
- $\varepsilon \in (C^1(\mathbb{R}^d))^d$ with $\|\varepsilon\| < 1$,

where $\|\cdot\|$ stands for the $(W^{1,\infty}(\mathbb{R}^d))^d$ norm

$$\|\cdot\| = \|\cdot\|_{L^\infty(\mathbb{R}^d))^d} + \|\nabla \cdot\|_{(L^\infty(\mathbb{R}^d))^{d\times d}}.$$

To prove the continuity of the far–field with respect to the obstacle, we first establish this result for the scattered field. Define $\widetilde{\lambda}_\varepsilon = \lambda \circ f_\varepsilon^{-1}$ and $\widetilde{\mu}_\varepsilon = \mu \circ f_\varepsilon^{-1}$ two elements of $L^\infty(\partial D_\varepsilon)$. To evaluate the distance between the solution u of $\mathcal{P}(\lambda, \mu, \partial D)$ and the solution u_ε of $\mathcal{P}(\widetilde{\lambda}_\varepsilon, \widetilde{\mu}_\varepsilon, \partial D_\varepsilon)$ we first transport u_ε on the fixed domain Ω_R by using a diffeomorphism between $\Omega_R^\varepsilon := \Omega_R \setminus \overline{D_\varepsilon}$ and Ω_R. Let $R_1 > 0$ be such that $\forall \varepsilon$ satisfying ($\mathcal{H}3$) $D_\varepsilon \subset B_{R_1}$ and $R_2 > R_1$ sufficiently large (see remark 3.2) such that there exists a $C^\infty(\mathbb{R}^d)$ cut-off function ψ such that

- ψ is compactly supported in B_{R_2},
- $\psi = 1$ on B_{R_1} and
- $\|\psi\|_{W^{1,\infty}(\mathbb{R}^d)} < 1$.

Then $Id + \psi\varepsilon$ is a C^1–diffeomorphism satisfying $(Id + \psi\varepsilon)(\Omega_R) = \Omega_R^\varepsilon$. We shall still denote by f_ε this diffeomorphism. From now on we take $R := R_2$ in the formulation (2).

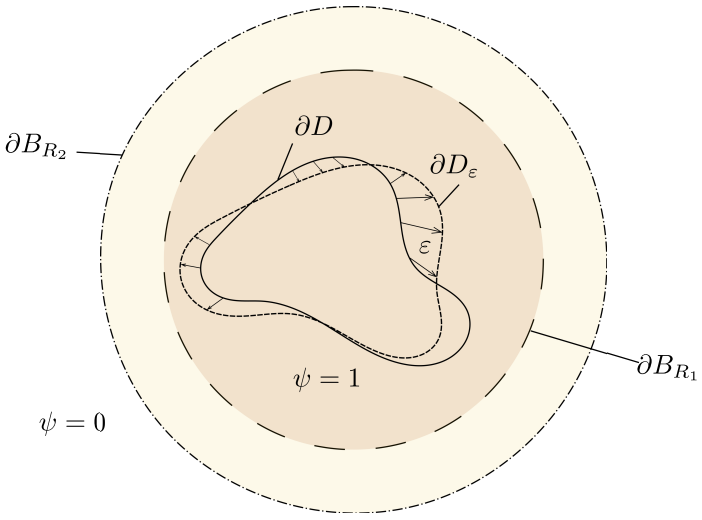

Figure 3: *Example of definition of the cut-off function ψ.*

Remark 3.2. *Let R_0 be the smallest real number such that $D \subset B_{R_0}$. Assumption $(\mathcal{H}3)$ implies that $\|\varepsilon\|_{L^\infty(\partial D)} < 1$ and taking $R_1 = 2R_0$ ensures that $D_\varepsilon \subset B_{R_1}$ for all suitable ε. If $R_2 = R_1 + 3$ we can construct a cut–off function satisfying the conditions above. Moreover, ψ depends only on the obstacle ∂D.*

Define $\widetilde{u}_\varepsilon := u_\varepsilon \circ f_\varepsilon$ where u_ε is the solution of $\mathcal{P}(\widetilde{\lambda}_\varepsilon, \widetilde{\mu}_\varepsilon, \partial D_\varepsilon)$, then the following estimate holds.

Theorem 3.3. *Let (λ, μ) be in K. Suppose that $(\mathcal{H}3)$ is satisfied, there exists two constants $\varepsilon_0 > 0$ and C_K which depend only on K such that for every $\|\varepsilon\| \leq \varepsilon_0$ we have:*

$$\|\widetilde{u}_\varepsilon - u\|_{H^1(\Omega_R)} \leq C_K \|\varepsilon\|. \tag{7}$$

We denote by $O(y)$ a $C^\infty(\mathbb{R})$ function such that

$$|O(y)| \leq C|y| \qquad \forall y \in \mathbb{R} \tag{8}$$

for $C > 0$ independent of y. In the proof of the Theorem we will need the following technical Lemma whose proof is postponed to the end of the Theorem's proof.

Lemma 3.4. *There exists a constant $C > 0$ such that for every ε satisfying $(\mathcal{H}3)$ and for every u, v in $H^1(\partial D)$ and $\mu \in L^\infty(\partial D)$ we have*

$$\left| \int_{\partial D_\varepsilon} (\mu \circ f_\varepsilon^{-1}) \nabla_{\partial D_\varepsilon} (u \circ f_\varepsilon^{-1}) \cdot \nabla_{\partial D_\varepsilon} (v \circ f_\varepsilon^{-1}) ds_\varepsilon - \int_{\partial D} \mu \nabla_{\partial D} u \cdot \nabla_{\partial D} v ds \right| \leq C \|u\|_{H^1(\partial D)} \|v\|_{H^1(\partial D)} \|\mu\|_{L^\infty(\partial D)} \|\varepsilon\|.$$

Proof of Theorem 3.3. The weak formulation of $\mathcal{P}(\widetilde{\lambda}_\varepsilon, \widetilde{\mu}_\varepsilon, \partial D_\varepsilon)$ is : find $u_\varepsilon \in V_R^\varepsilon := \{v \in H^1(\Omega_R^\varepsilon);\, v_{|\partial D_\varepsilon} \in H^1(\partial D_\varepsilon)\}$ such that for all $v_\varepsilon \in V_R^\varepsilon$ we have :

$$a_\varepsilon(u_\varepsilon, v_\varepsilon) = l_\varepsilon(v_\varepsilon)$$

with

$$\begin{aligned} a_\varepsilon(u_\varepsilon, v_\varepsilon) &= \int_{\Omega_R^\varepsilon} (\nabla u_\varepsilon \cdot \nabla \overline{v}_\varepsilon - k^2 u_\varepsilon \overline{v}_\varepsilon) dx_\varepsilon \\ &\quad + \int_{\partial D_\varepsilon} (\widetilde{\mu}_\varepsilon \nabla_{\partial D_\varepsilon} u_\varepsilon \cdot \nabla_{\partial D_\varepsilon} \overline{v}_\varepsilon - \widetilde{\lambda}_\varepsilon u_\varepsilon \overline{v}_\varepsilon) ds_\varepsilon - \langle S_R u_\varepsilon, v_\varepsilon \rangle \end{aligned}$$

$$l_\varepsilon(v_\varepsilon) = \int_{\partial B_R} \left(\frac{\partial u^i}{\partial r} - S_R(u^i) \right) \overline{v_\varepsilon} ds$$

We define a new bilinear form on V_R

$$\widetilde{a}_\varepsilon(u, v) := a_\varepsilon(u \circ f_\varepsilon^{-1}, v \circ f_\varepsilon^{-1}) \quad \forall u,\, v \in V_R.$$

As $f_\varepsilon(\partial B_R) = \partial B_R$, we have $l(v) = l_\varepsilon(v \circ f_\varepsilon^{-1})$ and $\widetilde{u}_\varepsilon$ is solution of

$$\widetilde{a}_\varepsilon(\widetilde{u}_\varepsilon, v) = l(v) \quad \forall v \in V_R.$$

In addition for every $v \in V_R$

$$S_R v = S_R(v \circ f_\varepsilon^{-1})$$

and as a consequence for every $u, v \in V_R$ we have $\langle S_R u, v \rangle = \langle S_R(u \circ f_\varepsilon^{-1}), v \circ f_\varepsilon^{-1} \rangle$. Using the change of variables formula for integrals (see chap. 5 of [11]), we have :

$$\begin{aligned} \widetilde{a}_\varepsilon(u, v) &= \int_{\Omega_R} (\nabla u \cdot P_\varepsilon \cdot \nabla \overline{v} - k^2 u\, \overline{v}) J_\varepsilon dx \\ &\quad + \int_{\partial D_\varepsilon} \widetilde{\mu}_\varepsilon [\nabla_{\partial D_\varepsilon}(u \circ f_\varepsilon^{-1})] \cdot [\nabla_{\partial D_\varepsilon}(\overline{v \circ f_\varepsilon^{-1}})] ds_\varepsilon \\ &\quad - \int_{\partial D} \lambda u\, \overline{v} J_\varepsilon^\nu ds - \langle S_R u, v \rangle \end{aligned}$$

where

- $J_\varepsilon = |det(\nabla f_\varepsilon)|$, where *det* stands for the determinant of a matrix,
- P_ε is the matrix $(\nabla f_\varepsilon)^{-1}(\nabla f_\varepsilon)^{-T}$,
- $J_\varepsilon^\nu = J_\varepsilon \left| (\nabla f_\varepsilon)^{-T} \nu \right|$

where for any invertible matrix B, B^{-T} is the transposition of the inverse of B. Thanks to Neumann series, we have the following development for $(\nabla f_\varepsilon(x))^{-1} = (Id + \nabla \varepsilon(x))^{-1}$ uniformly for $x \in \partial D$

$$(\nabla f_\varepsilon)^{-1}(x) = \sum_{n=0}^{\infty} (-1)^n (\nabla \varepsilon(x))^n = (1 + O(\|\varepsilon\|)) Id.$$

As a consequence $P_\varepsilon(x)$ expands uniformly for $x \in \partial D$ as

$$P_\varepsilon(x) = Id(1 + O(\|\varepsilon\|))$$

and we also have

$$J_\varepsilon(x) = 1 + O(\|\varepsilon\|) \quad \text{and} \quad J_\varepsilon^\nu(x) = 1 + O(\|\varepsilon\|)$$

since $det(Id+\nabla\varepsilon(x)) = 1+div(\varepsilon)+O(\|\varepsilon\|^2)$. Using all these results and Lemma 3.4 we are able to prove that the difference between the bilinear forms $\widetilde{a}_\varepsilon$ and a is small. For u and v two functions of V_R we have

$$\left|\int_{\Omega_R}(\nabla u\cdot P_\varepsilon\cdot\nabla\overline{v}J_\varepsilon - k^2u\,\overline{v}J_\varepsilon - \nabla u\cdot\nabla\overline{v}+k^2u\,\overline{v})dx\right| \le C\|u\|_{V_R}\|v\|_{V_R}\|\varepsilon\|$$

$$\left|\int_{\partial D}\{\lambda u\,\overline{v}J_\varepsilon^\nu - \lambda u\,\overline{v}\}ds\right| \le C\|\lambda\|_{L^\infty(\partial D)}\|u\|_{V_R}\|v\|_{V_R}\|\varepsilon\|$$

$$\left|\int_{\partial D_\varepsilon}(\mu\circ f_\varepsilon^{-1})\nabla_{\partial D_\varepsilon}(u\circ f_\varepsilon^{-1})\cdot\nabla_{\partial D_\varepsilon}(v\circ f_\varepsilon^{-1})ds_\varepsilon - \int_{\partial D}\mu\nabla_{\partial D}u\cdot\nabla_{\partial D}vds\right| \le C\|u\|_{V_R}\|v\|_{V_R)}\|\mu\|_{L^\infty(\partial D)}\|\varepsilon\|.$$

where the constant C does not depend on ε. One obtains for the bilinear forms $\widetilde{a}_\varepsilon$ and a:

$$|\widetilde{a}_\varepsilon(u,v)-a(u,v)| \le C_K\|u\|_{V_R}\|v\|_{V_R}\|\varepsilon\| \tag{9}$$

where C_K does not depend on λ, μ and ε. Thanks to the Riesz representation theorem we uniquely define A_ε from V_R into itself by

$$(A_\varepsilon v,w)_{V_R} = \widetilde{a}_\varepsilon(v,w) \quad \forall\, v,w\ \in V_R.$$

We recall the definition of the operator A of V_R

$$(Av,w)_{V_R} = a(v,w) \quad \forall v,w\in V_R$$

and of the element F of V_R

$$(F,w)_{V_R} = l(w) \quad \forall w\in V_R.$$

Thanks to inequality (9), we have

$$|||A_\varepsilon - A||| \le C_K\|\varepsilon\|.$$

To have information on the scattered field we should have information on the inverse of the operators and we will use once again the results on Neumann series of [13]. Actually, as soon as $|||A^{-1}(A_\varepsilon - A)||| \le 1/2$ which is true when $\varepsilon_0 \le 1/(2C_K^2)$ (see Proposition 2.2), the inverse operator of A_ε satisfies

$$|||A_\varepsilon^{-1}||| \le \frac{|||A^{-1}|||}{1-|||A^{-1}(A_\varepsilon - A)|||} \le 2C_K.$$

From the identity $\widetilde{u}_\varepsilon - u = A_\varepsilon^{-1}(A-A_\varepsilon)u$ we deduce

$$\begin{aligned}\|\widetilde{u}_\varepsilon - u\|_{V_R} &= \|A_\varepsilon^{-1}((A-A_\varepsilon)u)\|_{V_R}\\ &\le |||A_\varepsilon^{-1}|||||(A_\varepsilon - A)u\|_{V_R}\\ &\le 2C_K^2\|\varepsilon\|\|u\|_{V_R} \le 2C_K^3\|\varepsilon\|\|F\|_{V_R}\end{aligned}$$

where we again used Proposition 2.2 for the last inequality. This provides the desired estimate. □

Proof of Lemma 3.4. Let us consider three functions $u \in H^1(\partial D)$, $v \in H^1(\partial D)$ and $\mu \in L^\infty(\partial D)$ and let $x_0 \in \partial D$. There exists a function φ of class C^1 and an open set $U \subset \mathbb{R}^{d-1}$ such that

$$\partial D \cap V = \{\varphi(\xi)\ ;\ \xi \in U\}$$

where V is a neighbourhood of x_0 and $\varphi(0) = x_0$ and such that

$$e_i := \frac{\partial \varphi}{\partial \xi_i}(0)\ ,\ \text{for } i = 1, d-1$$

form a basis of the tangential plane to ∂D at x_0. We can also use this parametrization to describe a surfacic neighbourhood of $x_{0,\varepsilon} := f_\varepsilon(x_0)$, similarly there exists a neighbourhood V_ε of $x_{0,\varepsilon}$ such that

$$\partial D_\varepsilon \cap V_\varepsilon = \{\varphi_\varepsilon(\xi)\ ;\ \xi \in U\}$$

where $\varphi_\varepsilon := f_\varepsilon \circ \varphi$. We define the tangential vectors of ∂D_ε at point $x_{0,\varepsilon} = \varphi_\varepsilon(0)$ by

$$e_{\varepsilon,i} := \frac{\partial \varphi_\varepsilon}{\partial \xi_i}(0)\ \text{ for } i = 1, d-1$$

and thanks to the chain rule

$$e_{\varepsilon,i} = \nabla f_\varepsilon(x_0) e_i. \tag{10}$$

Remark that as $\nabla f_\varepsilon(x_0)$ is an invertible matrix ($\|\varepsilon\| < 1$), the family $e_{\varepsilon,i}$ is a basis of the tangent plane to ∂D_ε at $x_{\varepsilon,0}$. Finally, we define the covariant basis of the cotangent planes of ∂D at point x_0 and of ∂D_ε at point $x_{0,\varepsilon}$ by

$$e^i \cdot e_j = \delta^i_j\ \text{ and }\ e^i_\varepsilon \cdot e_{\varepsilon,j} = \delta^i_j \quad \text{for } i, j = 1, d-1.$$

Using this definition and (10) we have the relation

$$e^i_\varepsilon = (\nabla f_\varepsilon)^{-T} e^i \quad i = 1, d-1.$$

Finally in the covariant basis, the tangential gradient $\nabla_{\partial D}$ for $w \in H^1(\partial D)$ at point x_0 is

$$\nabla_{\partial D} w(x_0) = \sum_{i=1}^{d-1} \frac{\partial \widetilde{w}}{\partial \xi_i}(0) e^i$$

where $\widetilde{w} := w \circ \varphi$. Similarly, at point $x_{0,\varepsilon}$ we have for $w_\varepsilon \in H^1(\partial D_\varepsilon)$

$$\nabla_{\partial D_\varepsilon} w_\varepsilon(x_{0,\varepsilon}) = \sum_{i=1}^{d-1} \frac{\partial \widetilde{w}_\varepsilon}{\partial \xi_i}(0) e^i_\varepsilon$$

where $\widetilde{w}_\varepsilon := w_\varepsilon \circ \varphi_\varepsilon$. As a consequence, for $w \in H^1(\partial D)$

$$\begin{aligned}
\nabla_{\partial D_\varepsilon}(w \circ f_\varepsilon^{-1})(x_{0,\varepsilon}) &= \sum_{i=1}^{d-1} \frac{\partial \widetilde{w}}{\partial \xi_i}(0) e^i_\varepsilon \\
&= \sum_{i=1}^{d-1} \frac{\partial \widetilde{w}}{\partial \xi_i}(0) (\nabla f_\varepsilon(x_0))^{-T} e^i \\
&= (\nabla f_\varepsilon(x_0))^{-T} \nabla_{\partial D} w(x_0)
\end{aligned}$$

because $w \circ f_\varepsilon^{-1} \circ \varphi_\varepsilon = \widetilde{w}$. By this formula, we just proved that for every $x_\varepsilon = f_\varepsilon(x)$, $x \in \partial D$ we have

$$\nabla_{\partial D_\varepsilon}(w \circ f_\varepsilon^{-1})(x_\varepsilon) = (\nabla f_\varepsilon(x))^{-T} \nabla_{\partial D} w(x) \tag{11}$$

for every $w \in H^1(\partial D)$. For u, v and μ, change of variables in the boundary integral ($x = f_\varepsilon^{-1}(x_\varepsilon)$) gives

$$\begin{aligned}\int_{\partial D_\varepsilon} &(\mu \circ f_\varepsilon^{-1}) \nabla_{\partial D_\varepsilon}(u \circ f_\varepsilon^{-1}) \cdot \nabla_{\partial D_\varepsilon}(v \circ f_\varepsilon^{-1}) dx_\varepsilon \\ &= \int_{\partial D} \mu(x) [\nabla_{\partial D_\varepsilon}(u \circ f_\varepsilon^{-1})(f_\varepsilon(x))] \cdot [\nabla_{\partial D_\varepsilon}(v \circ f_\varepsilon^{-1})(f_\varepsilon(x))] J_\varepsilon^\nu dx\end{aligned}$$

and thanks to the relation (11)

$$\begin{aligned}\int_{\partial D_\varepsilon} &(\mu \circ f_\varepsilon^{-1}) \nabla_{\partial D_\varepsilon}(u \circ f_\varepsilon^{-1}) \cdot \nabla_{\partial D_\varepsilon}(v \circ f_\varepsilon)^{-1} dx_\varepsilon \\ &= \int_{\partial D} \mu(x) [\nabla_{\partial D} u(x)] (\nabla f_\varepsilon(x))^{-1} (\nabla f_\varepsilon(x))^{-T} [\nabla_{\partial D} v(x)] J_\varepsilon^\nu dx.\end{aligned}$$

Finally recalling that

$$(\nabla f_\varepsilon(x))^{-1}(\nabla f_\varepsilon(x))^{-T} = P_\varepsilon(x) = (1 + O(\|\varepsilon\|))Id \quad \text{and} \quad J_\varepsilon^\nu = 1 + O(\|\varepsilon\|)$$

we may write

$$\begin{aligned}\int_{\partial D_\varepsilon} &(\mu \circ f_\varepsilon^{-1}) \nabla_{\partial D_\varepsilon}(u \circ f_\varepsilon^{-1}) \cdot \nabla_{\partial D_\varepsilon}(v \circ f_\varepsilon^{-1}) dx_\varepsilon \\ &= (1 + O(\|\varepsilon\|)) \int_{\partial D} \mu \nabla_{\partial D} u \cdot \nabla_{\partial D} v dx\end{aligned}$$

which is the desired result. □

Corollary 3.5. *Let (λ, μ) be in K. Suppose that $(\mathcal{H}3)$ is satisfied, there exists two constants $\varepsilon_0 > 0$ and C_K which depend only on K such that for every $\|\varepsilon\| \leq \varepsilon_0$ we have:*

$$\|T(\lambda \circ f_\varepsilon^{-1}, \mu \circ f_\varepsilon^{-1}, \partial D_\varepsilon) - T(\lambda, \mu, \partial D)\|_{L^2(S^{d-1})} \leq C_K \|\varepsilon\|.$$

Proof. Let u^∞ be the far–field that corresponds to the obstacle D and u_ε^∞ the one that corresponds to the obstacle D_ε. We now write the integral representation formula for the far–field on ∂B_R and as $\widetilde{u}_\varepsilon|_{\partial B_R} = u_\varepsilon|_{\partial B_R}$ we obtain

$$u_\varepsilon^\infty(\hat{x}) \;=\; \int_{\partial B_R} \left(\widetilde{u}_\varepsilon(y) \frac{\partial \widetilde{\Phi}^\infty(y, \hat{x})}{\partial \nu(y)} - \frac{\partial \widetilde{u}_\varepsilon(y)}{\partial \nu} \widetilde{\Phi}^\infty(y, \hat{x}) \right) ds(y)\,.$$

We know that the exterior DtN map defined in section 2 is continuous from $H^{1/2}(\partial B_R)$ to $H^{-1/2}(\partial B_R)$ and as a consequence

$$\left\| \frac{\partial \widetilde{u}_\varepsilon}{\partial \nu} \right\|_{H^{-1/2}(\partial B_R)} \leq C \|\widetilde{u}_\varepsilon\|_{H^{1/2}(\partial B_R)}\,,$$

finally

$$\|u_\varepsilon^\infty(\hat{x}) - u^\infty(\hat{x})\|_{L^2(S^{d-1})} \leq C\|\widetilde{u}_\varepsilon - u\|_{H^{1/2}(\partial B_R)}\,.$$

The trace is continuous from $H^1(\Omega_R)$ into $H^{1/2}(\partial B_R)$ so we combine this last inequality with (7) to obtain the continuity result

$$\|T(\lambda \circ f_\varepsilon^{-1}, \mu \circ f_\varepsilon^{-1}, \partial D_\varepsilon) - T(\lambda, \mu, \partial D)\|_{L^2(S^{d-1})} \leq C_K\|\varepsilon\|\,.$$

□

This ends the first step of the stability result. In the next section we use this continuity result and the stability assumption of section 2.2 to prove a stability estimate with respect to the obstacle.

3.3 Conclusion

In this section we assume that we satisfy $(\mathcal{H}2)$ for a given K and $(\mathcal{H}3)$.

Theorem 3.6. *There exists a constant ε_0 which depends only on K such that for every $(\lambda, \mu) \in K$ there exists a constant $C(\lambda, \mu, K)$ such that for every $\|\varepsilon\| \leq \varepsilon_0$ and for every $(\lambda_\varepsilon \circ f_\varepsilon, \mu_\varepsilon \circ f_\varepsilon) \in K$ that satisfy*

$$\|T(\lambda_\varepsilon, \mu_\varepsilon, \partial D_\varepsilon) - T(\lambda, \mu, \partial D)\|_{L^2(S^{d-1})} \leq \delta \quad \text{for } \delta > 0$$

we have

$$\|\lambda_\varepsilon \circ f_\varepsilon - \lambda\|_{L^\infty(\partial D)} + \|\mu_\varepsilon \circ f_\varepsilon - \mu\|_{L^\infty(\partial D)} \leq C(\lambda, \mu, K)(\delta + \|\varepsilon\|).$$

Proof. The idea of the proof is to split the uniform continuity with respect to the obstacle and the stability with respect to the coefficients and to use assumption $(\mathcal{H}2)$. The aim is to prove that

$$\|T(\lambda_\varepsilon \circ f_\varepsilon, \mu_\varepsilon \circ f_\varepsilon, \partial D) - T(\lambda, \mu, \partial D)\|_{L^2(S^{d-1})} \leq g(\delta, \|\varepsilon\|)$$

for a suitable g. We have

$$\begin{aligned}\|T(\lambda_\varepsilon \circ f_\varepsilon, \mu_\varepsilon \circ f_\varepsilon, \partial D) - T(\lambda, \mu, \partial D)\|_{L^2(S^{d-1})} \\ \leq \|T(\lambda_\varepsilon, \mu_\varepsilon, \partial D_\varepsilon) - T(\lambda_\varepsilon \circ f_\varepsilon, \mu_\varepsilon \circ f_\varepsilon, \partial D)\|_{L^2(S^{d-1})} \\ + \|T(\lambda, \mu, \partial D) - T(\lambda_\varepsilon, \mu_\varepsilon, \partial D_\varepsilon)\|_{L^2(S^{d-1})}\end{aligned}$$

but the hypothesis of the Theorem tells us that

$$\|T(\lambda_\varepsilon, \mu_\varepsilon, \partial D_\varepsilon) - T(\lambda, \mu, \partial D)\|_{L^2(S^{d-1})} \leq \delta$$

and as we have continuity with respect to the obstacle (see Corollary 3.5) we have

$$\|T(\lambda_\varepsilon, \mu_\varepsilon, \partial D_\varepsilon) - T(\lambda_\varepsilon \circ f_\varepsilon, \mu_\varepsilon \circ f_\varepsilon, \partial D)\|_{L^2(S^{d-1})} \leq C_K\|\varepsilon\|$$

because we took $\lambda_\varepsilon \circ f_\varepsilon$ and $\mu_\varepsilon \circ f_\varepsilon$ in a given compact set K. Finally we have

$$\|T(\lambda_\varepsilon \circ f_\varepsilon, \mu_\varepsilon \circ f_\varepsilon, \partial D) - T(\lambda, \mu, \partial D)\|_{L^2(S^{d-1})} \leq C_K(\delta + \|\varepsilon\|)$$

and the stability assumption in $(\mathcal{H}2)$ tells us that

$$\begin{aligned}\|\lambda_\varepsilon \circ f_\varepsilon - \lambda\|_{L^\infty(\partial D)} + \|\mu_\varepsilon \circ f_\varepsilon - \mu\|_{L^\infty(\partial D)} \\ \leq C(\lambda, \mu, K)\|T(\lambda_\varepsilon \circ f_\varepsilon, \mu_\varepsilon \circ f_\varepsilon, \partial D) - T(\lambda, \mu, \partial D)\|_{L^2(S^{d-1})}\end{aligned}$$

which concludes the proof. □

Remark 3.7. *The local nature of this estimate only depends on the local stability result for the impedances. In the case of a classic impedance boundary condition ($\mu = 0$) we could use the global stability results of Sincich in [18] or of Labreuche in [14] and obtain a constant $C(\lambda, \mu, K)$ that only depends on K.*

4 Numerical algorithm and experiments

This section is dedicated to the effective reconstruction of the impedance functional coefficients λ and μ from the observed far–field $u^\infty_{obs} \in L^2(S^{d-1})$ associated to a given incident direction and a given obstacle. In this view we shall minimize the cost function

$$F(\lambda, \mu) = \frac{1}{2}\|T(\lambda, \mu) - u^\infty_{obs}\|^2_{L^2(S^{d-1})} \tag{12}$$

with respect to λ and μ using a steepest descent method.

4.1 Fréchet derivative of the cost function

First of all, to minimize the cost function F, we have to compute its Fréchet derivative and hence to calculate the Fréchet derivative of the far–field map T.

Lemma 4.1. *The far–field map T is Fréchet differentiable and for $(\lambda, \mu) \in (L^\infty(\partial D))^2$ that satisfy $(\mathcal{H}1)$ its Fréchet derivative $dT_{\lambda,\mu} : L^\infty(\partial D)^2 \to L^2(S^{d-1})$ maps (h, l) to $v^\infty_{h,l}$ such that*

$$v^\infty_{h,l}(\hat{x}) := \langle p(., \hat{x}), div_{\partial D}(l\nabla_{\partial D} u) + hu\rangle_{H^1(\partial D), H^{-1}(\partial D)}, \quad \forall \hat{x} \in S^{d-1},$$

where u is the solution of (1) and $p(., \hat{x})$ is the solution of problem (1) in which u^i is replaced by $\Phi^\infty(., \hat{x})$.

Proof. Following the proof of Proposition 6 in [3], we obtain that T is differentiable and that $dT_{\lambda,\mu}(h, l) = v^\infty_{h,l}$ where $v^\infty_{h,l}$ is the far–field associated with $v^s_{h,l}$ solution of

$$\begin{cases} \Delta v^s_{h,l} + k^2 v^s_{h,l} = 0 \quad \text{in } \Omega \\ \mathrm{div}_{\partial D}(\mu \nabla_{\partial D} v^s_{h,l}) + \dfrac{\partial v^s_{h,l}}{\partial \nu} + \lambda v^s_{h,l} = -\mathrm{div}_{\partial D}(l\nabla_{\partial D} u) - hu \quad \text{on } \partial D \\ \lim\limits_{R\to\infty} \displaystyle\int_{\partial B_R} |\partial v^s_{h,l}/\partial r - ikv^s_{h,l}|^2 ds = 0\,. \end{cases} \tag{13}$$

From (5), we have for all $\hat{x} \in S^{d-1}$

$$v^\infty_{h,l}(\hat{x}) = \int_{\partial D} \left(v^s_{h,l} \frac{\partial \Phi^\infty(., \hat{x})}{\partial \nu} - \frac{\partial v^s_{h,l}}{\partial \nu} \Phi^\infty(., \hat{x}) \right) ds. \tag{14}$$

Since on ∂D

$$\frac{\partial v^s_{h,l}}{\partial \nu} + \mathrm{div}_{\partial D}(\mu \nabla_{\partial D} v^s_{h,l}) + \lambda v^s_{h,l} = -\mathrm{div}_{\partial D}(l\nabla_{\partial D} u) - hu$$

replacing $Dv^s_{h,l}$ in (14) and integrating by part we obtain

$$v^\infty_{h,l}(\hat{x}) = \left\langle v^s_{h,l}, \mathrm{div}_{\partial D}(\mu\nabla_{\partial D}\Phi^\infty(.,\hat{x})) + \frac{\partial\Phi^\infty(.,\hat{x})}{\partial\nu} + \lambda\Phi^\infty(.,\hat{x})\right\rangle_{H^1(\partial D),H^{-1}(\partial D)} + \langle\Phi^\infty(.,\hat{x}), \mathrm{div}_{\partial D}(l\nabla_{\partial D}u) + hu\rangle_{H^1(\partial D),H^{-1}(\partial D)} \,. \tag{15}$$

We introduce $p(\cdot,\hat{x})$, the adjoint state solution of (1) with $u^i = \Phi^\infty(\cdot,\hat{x})$. $p^s(\cdot,\hat{x}) := p(\cdot,\hat{x}) - \Phi^\infty(\cdot,\hat{x})$ satisfies on ∂D

$$\mathrm{div}_{\partial D}(\mu\nabla_{\partial D}p^s) + \frac{\partial p^s}{\partial\nu} + \lambda p^s = -\mathrm{div}_{\partial D}(\mu\nabla_{\partial D}\Phi^\infty) - \frac{\partial\Phi^\infty}{\partial\nu} - \lambda\Phi^\infty \,.$$

As $v^s_{h,l}$ and p^s are radiating solutions of a scattering problem the following identity holds:

$$\int_{\partial D}\left(\frac{\partial p^s}{\partial\nu}v^s_{h,l} - p^s\frac{\partial v^s_{h,l}}{\partial\nu}\right)ds = 0\,,$$

finally using the boundary condition for p^s and then for $v^s_{h,l}$, equation (15) becomes

$$\begin{aligned} v^\infty_{h,l}(\hat{x}) &= -\left\langle p^s(\cdot,\hat{x}), \mathrm{div}_{\partial D}(\mu\nabla_{\partial D}v^s_{h,l} + \frac{\partial v^s_{h,l}}{\partial\nu(y)} + \lambda v^s_{h,l})\right\rangle_{H^1(\partial D),H^{-1}(\partial D)} \\ &\quad + \langle\Phi^\infty(.,\hat{x}), \mathrm{div}_{\partial D}(l\nabla_{\partial D}u) + hu\rangle_{H^1(\partial D),H^{-1}(\partial D)} \\ &= \langle p(.,\hat{x}), \mathrm{div}_{\partial D}(l\nabla_{\partial D}u) + hu\rangle_{H^1(\partial D),H^{-1}(\partial D)} \end{aligned}$$

which concludes the proof. □

Theorem 4.2. *The function F is differentiable and for $(\lambda,\mu) \in (L^\infty(\partial D))^2$ that satisfy $(\mathcal{H}1)$ its Fréchet derivative satisfies*

$$\forall (h,l) \in (L^\infty(\partial D))^2 \quad dF(\lambda,\mu)\cdot(h,l) = \Re e\,\langle G, div_{\partial D}(l\nabla_{\partial D}u) + hu\rangle_{H^1(\partial D),H^{-1}(\partial D)}$$

where

- *u is the solution of the problem $\mathcal{P}(\lambda,\mu,\partial D)$,*
- *$G = G^i + G^s$ is the solution of $\mathcal{P}(\lambda,\mu,\partial D)$ with u^i replaced by*

$$G^i(y) := \int_{S^{d-1}}\Phi^\infty(y,\hat{x})\overline{(T(\lambda,\mu) - u^\infty_{obs})}d\hat{x}.$$

Proof. By composition of derivatives and using the Fubini theorem we have for $(h,l) \in L^\infty(\partial D)^2$

$$\begin{aligned} dF(\lambda,\mu)\cdot(h,l) &= \Re e\left\{(T(\lambda,\mu) - u^\infty_{obs}, dT(\lambda,\mu)\cdot(h,l))_{L^2(S^{d-1})}\right\} \\ &= \Re e\int_{S^{d-1}}\left\{\overline{(T(\lambda,\mu) - u^\infty_{obs})}(\hat{x})\,\langle p(y,\hat{x}), A(u)(y)\rangle_{H^1(\partial D),H^{-1}(\partial D)}\right\}d\hat{x} \\ &= \Re e\,\langle G, A(u)\rangle_{H^1(\partial D),H^{-1}(\partial D)} \end{aligned}$$

with

$$A(u)(y) = \mathrm{div}_{\partial D}(l(y)\nabla_{\partial D}u(y)) + h(y)u(y).$$

□

4.2 Numerical algorithm

To minimize the cost function (12) we use a steepest descent method and we calculate the gradient of F with the help of Lemma 4.1. We solve the direct problems using a finite elements method (implemented with FreeFem++ [21]) with a truncated DtN map on the boundary of a circle of sufficiently large radius R, in order to bound the computational domain. We will consider different geometries for the obstacle D and we look for the imaginary part of a function λ with $\Im m(\lambda) \geq 0$ and the real part of a function μ with $\Re e(\mu)(x) \geq c > 0$ for almost every $x \in \partial D$ assuming that $\Re e(\lambda)$ and $\Im m(\mu)$ are known in order to satisfy hypothesis presented in [3] for which uniqueness and stability hold. Moreover, for sake of simplicity we will choose these known parts of the impedances equal to zero. Let us give initial values λ_{init} and μ_{init} in the same finite element space as the one used to solve the forward problem. We update these values at each time step n as follows

$$\lambda_{n+1} = \lambda_n - i\delta\lambda_n$$

where the descent direction $\delta\lambda_n$ is taken proportional to $dF(\lambda_n, \mu_n)$. Since the number of parameters for λ_n is in general high, a regularization of $dF(\lambda_n, \mu_n)$ is needed. We choose to use a $H^1(\partial D)$–regularization (see [1] for a similar regularization procedure) by taking $\delta\lambda_n \in H^1(\partial D)$ solution to

$$\eta_1(\nabla_{\partial D}(\delta\lambda_n), \nabla_{\partial D}\varphi)_{L^2(\partial D)} + (\delta\lambda_n, \varphi)_{L^2(\partial D)} = \alpha_1 dF(\lambda_n, \mu_n) \cdot (i\varphi, 0) \quad (16)$$

for each φ in the finite element space and with η_1 the regularization parameter to choose and α_1 is the descent coefficient for λ. We used $i\varphi$ in (16) in order to compute the gradient with respect to the imaginary part of λ. We apply a similar procedure for μ,

$$\mu_{n+1} = \mu_n - \delta\mu_n$$

where $\delta\mu_n$ solves

$$\eta_2(\nabla_{\partial D}(\delta\mu_n), \nabla_{\partial D}\varphi)_{L^2(\partial D)} + (\delta\mu_n, \varphi)_{L^2(\partial D)} = \alpha_2 dF(\lambda_n, \mu_n) \cdot (0, \varphi).$$

We take two different regularization parameters for λ and μ since we observed that the algorithm has different sensitivities with respect to each coefficient. From the practical point of view we choose large η_i at the first steps to quickly approximate the searched λ and μ then we decrease them during the algorithm in order to increase the precision of the reconstruction. In all the computations (except for constant λ and μ), the parameters α_1 and α_2 are chosen in such a way that the cost function decreases at each step. A more precise description of the algorithm is given in the following where `lambda` and `mu` respectively denote λ_n and μ_n at time step n.

First step (if $n > 0$): update λ and μ

- if n is even :

```
newmu = mu - alphamu*gradmu;
newlambda = lambda;
```

- if n is odd :

```
newlambda = lambda - alphalambda*gradlambda;
newmu = mu;
```

Second step: computation of the cost function `Fnew:=F(newlambda,newmu)`

- `solve the scattering problem for newlambda and newmu`
- `determine the associated far-field`
- `evaluate the new cost function newF`

Third step: validation

- `If newF > F`
  - if n is even `alphamu=alphamu/2;`
  - if n is odd `alphalambda=alphalambda/2;`
- `If newF < F`
  - `lambda = lambdanew; mu=munew;`
  - `F=Fnew;`
  - `compute gradmu and gradlambda` (evaluation of the adjoint state)
  - `alphamu = 2*alphamu (if n is even),`
    `alphalambda = 2*alphalambda; (if n is odd).`

Stopping criterion We stop the algorithm if the descent coefficients α_μ and α_λ are too small or if the number of iterations is larger than 100 (in every cases there was not a concrete improvement of the reconstruction after 80 iterations).

Remark that we update alternatively λ and μ because the cost function is much more sensitive to λ than to μ and as a consequence, if we update both at each time step, we would have a poor reconstruction of μ.

4.3 Numerical experiments

In this section we will show some numerical reconstructions using synthetic data generated with the code *FreeFem++* in two dimensions to highlight the importance of each parameter of the problem. The aim is to better understand the behaviour of the iterative algorithm we presented in the previous section. First of all, we will see that the use of a single incident wave is not satisfactory and we will quickly turn to the use of several incident waves. Then all the simulations will be done with several incident waves and with limited aperture data. Remark that all the theoretical results still hold in this particular case (see remark 2.3). In most of the simulations the obstacle will be an ellipse (see Figure 4) but we will show the influence of the convexity of the obstacle on the quality of the reconstruction. In most of experiments, the diameter of the obstacle will be more or less equal to the wavelength ($2\pi/k$). Moreover, since we consider a modelling of physical properties we rescale the equation on the boundary of the obstacle ∂D in order to deal with dimensionless coefficients λ and μ. The equation on ∂D becomes

$$\mathrm{div}_{\partial D}\left(\frac{\mu}{k}\nabla_{\partial D}u\right)+\frac{\partial u}{\partial \nu}+k\lambda u=0.$$

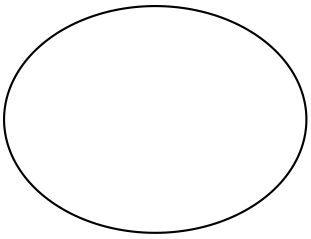

Figure 4: *Geometry of the obstacle,* $X(\theta) = (0.3\cos(\theta); 0.2\sin(\theta))$.

In all cases (except when we specify it), we simply reconstruct μ taking $\lambda = 0$ because the reconstruction of λ has been investigated for a long time (see [5] or more recently [6]). Finally, we will only consider star–shaped obstacles $\partial D = \{r = X(\theta),\ \theta \in [0, 2\pi[\}$ and so we can define the impedance functions as functions of the angle θ. In the following we will represent λ and μ with the help of such a parametrization.

4.3.1 A single incident wave with full aperture

In this section we consider the exact framework of the theory developed at the beginning, namely we enlighten the obstacle with a single incident plane

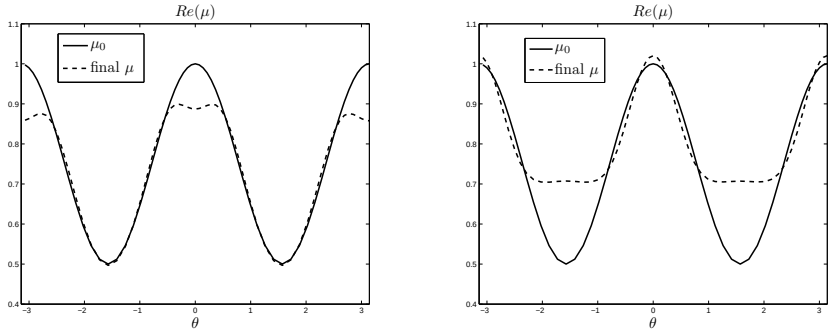

Figure 5: *Reconstruction of* $\Re e(\mu_0) = 0.5(1 + cos^2(\theta))$, $\lambda = 0$, $\mu_{init} = 0.7$, *wave number* $k = 9$, *the incident angle is* 0 *on the left and* $\pi/2$ *on the right.*

wave and we measure the far–field in all directions. As we could expect, the reconstruction is quite good in the enlightened area but rather poor far away from such area (see Figure 4.3.1).

4.3.2 Several incident waves and limited aperture

In this section we suppose that we measure several far–fields corresponding to several incident directions. We hence reproduce an experimental device (see Figure 6) that would rotate around the obstacle D. To be more specific, we denote $u^s(\cdot, d)$ the scattered field associated with the incident plane wave of

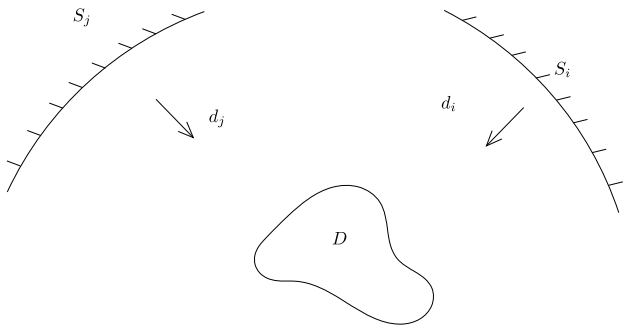

Figure 6: *Several limited observations.*

direction d. Considering we have N incident directions d_j and N areas of observation $S_j \subset S^1$ such that $\bigcup S_i = S^1$ and $S_i \cap S_j = \emptyset$ for $i \neq j$, we construct a new cost function

$$F(\lambda, \mu) \quad = \quad \frac{1}{2} \sum_{j=1}^{N} \|T(\lambda, \mu, d_j) - u_{obs}^{\infty}(\cdot, d_j)\|_{L^2(S_j)}^2 .$$

To minimize F we use the same technique as before but now the Herglotz incident wave G^i is associated with the incident direction d_j and is given by

$$G^i(y, d_j) = \int_{S_j} \Phi^{\infty}(y, \hat{x}) \overline{(T(\lambda, \mu) - u_{obs}^{\infty})} d\hat{x}.$$

More precisely, for the next experiments we send $N = 10$ incident waves that are uniformly distributed on the unit circle and the aperture of observation is of $\pi/5$ so that the global angle of observation is 2π. First of all let us show that this experimental setting provides more accurate results than the previous one.

Testing the accuracy of the algorithm. On Figure 4.3.2 we can see two reconstructions for two ranges of μ, $\mu \sim 1$ on the left and $\mu \sim 10$ on the right, we use exact data to verify that the algorithm converges and gives good results. Obviously, the results are much more accurate than in the case of a single incident wave. In order to evaluate the convergence of the algorithm, we introduce the following relative cost function:

$$\text{Error} \ := \frac{\sum_{i=1}^{N} \|T(\lambda, \mu, d_i) - u_{obs}^{\infty}(\cdot, d_i)\|_{L^2(S_i)}^2}{\sum_{i=1}^{N} \|u_{obs}^{\infty}(\cdot, d_i)\|_{L^2(S_i)}^2}.$$

The obtained relative error is really small ($< 1\%$) and is probably due to numerical errors on the far–field computation. From now on we will add some noise on the data to avoid "inverse crime". Precisely we handle some noisy data $u_{\sigma}^{\infty}(\cdot, d_i)$ such that

$$\frac{\|u_{\sigma}^{\infty}(\cdot, d_i) - u_{obs}^{\infty}(\cdot, d_i)\|_{L^2(S_i)}}{\|u_{obs}^{\infty}(\cdot, d_i)\|_{L^2(S_i)}} = \sigma .$$

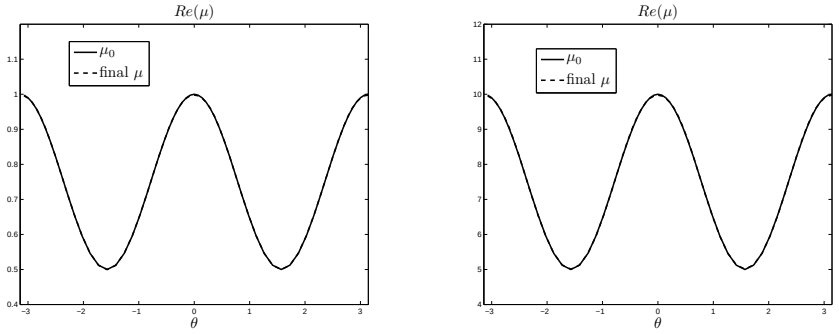

(a) Initial Error = 24%, Final Error = 0.03%

(b) Initial Error = 3887%, Final Error = 0.6%

Figure 7: *Wave number* $k = 9$*, regularization parameter* $\eta = 0$*,* $\lambda = 0$*, reconstruction of* $\Re e(\mu_0) = 0.5(1 + cos^2(\theta))$*,* $\mu_{init} = 0.7$ *on the left and* $\Re e(\mu_0) = 5(1 + cos^2(\theta))$*,* $\mu_{init} = 7$ *on the right.*

In the next experiments we study the impact of the level of noise (1% and 5%) on the quality of the reconstruction. $Error(\sigma)$ will denote the final error with amplitude of noise σ.

Influence of the wavelength and the regularization parameter. We are now interested in the influence of the wavelength on the accuracy of the results, the first two graphics (Figure 4.3.2) show how the algorithm behaves with respect to the wavelength. We can see that if we decrease the wavelength (Figure 8(b)) the reconstructed impedance is very irregular, that's why on Figure 8(c) we add some regularization to flatten the solution, and then improve the reconstruction. Note that if the wavelength is too small, all the tested regularization strategies did not allow us to correctly capture the solution (see Figure 8(c) with 5% noise).

The case of non–smooth functional coefficients. We are able to identify a non–smooth coefficient μ since μ is expressed as a linear combination of functions of the finite element space. We present our results on Figure 4.3.2 for piecewise constant functions μ. To have a good reconstruction of a piecewise constant function, we need a small wavelength. However, we have just seen before that too small wavelength generates instability due to the noise that contaminates data. That's why we use a two steps procedure. First we use a large wavelength equal to 0.7 ($k = 9$, on the left) to quickly find a good approximation of the coefficient. Secondly, to improve the result, we use a three times smaller wavelength ($k = 24$ on the right). Hence, we combine the advantage of a large wavelength (low numerical cost) and the advantage of a small wavelength (good precision on the reconstruction of the discontinuity). We clearly improve the result compared with the reconstruction using a wave number equal to 9.

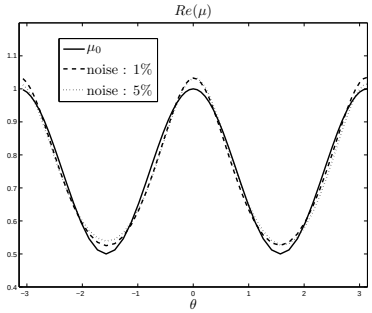

(a) Error (1%) = 2%, Error (5%) = 11%

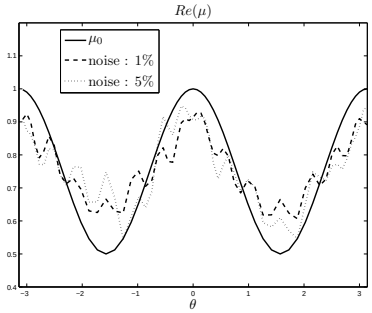

(b) Error (1%) = 2.8%, Error (5%) = 11.5%

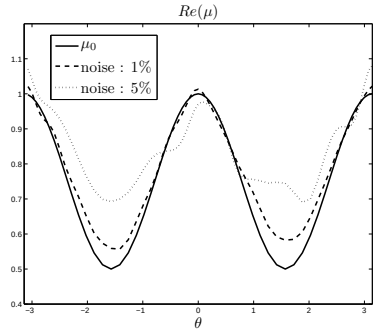

(c) Error (1%) = 2.1%, Error (5%) = 10.2%

Figure 8: *Reconstruction of* $\Re e(\mu_0) = 0.5(1 + cos^2(\theta))$, $\mu_{init} = 0.7$, $\lambda = 0$, *with no regularization procedure, wave number* $k = 2$ *(top left) and* $k = 24$ *(top right); with a regularization procedure and* $k = 24$ *(bottom).*

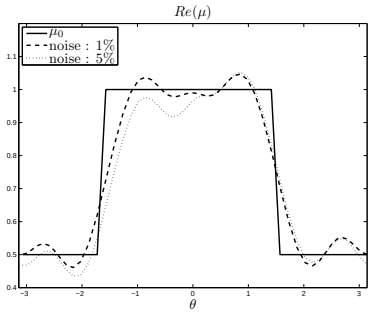

(a) Error (1%) = 2.9%, Error (5%) = 11.4%

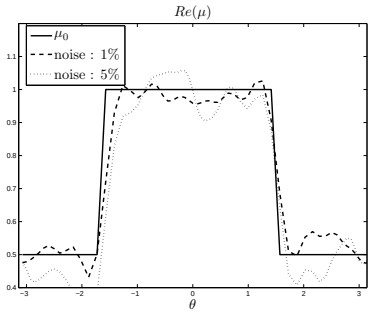

(b) Error (1%) = 2.3%, Error (5%) = 11%

Figure 9: *Reconstruction of* $\Re e(\mu_0) = 0.5 + 0.5\chi_{[-\pi/2,\pi/2]}$, $\mu_{init} = 0.7$, $\lambda = 0$, *the wave number is* $k = 9$ *on the left and* $k = 24$ *on the right.*

Influence of the non–convexity of the obstacle. The aim of this part is to study the influence of the non–convexity on the quality of the reconstruction.

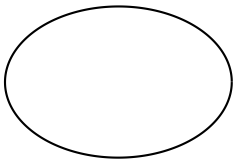

(a) $X(\theta) = (0.3\cos(\theta); 0.2\sin(\theta))$

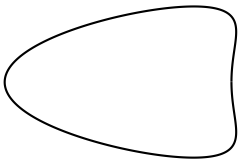

(b) $X(\theta) = (0.3\cos(\theta-\pi) + 0.1\cos(2(\theta-\pi)); 0.2\sin(\theta))$

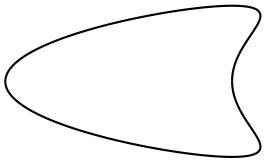

(c) $X(\theta) = (0.3\cos(\theta-\pi) + 0.15\cos(2(\theta-\pi)); 0.2\sin(\theta))$

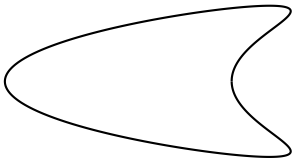

(d) $X(\theta) = (0.3\cos(\theta-\pi) + 0.2\cos(2(\theta-\pi)); 0.2\sin(\theta))$

Figure 10: *"Kite"–shaped obstacle.*

In this perspective, we consider four different geometries represented on Figure 10, and on Figure 4.3.2 we present the reconstruction of a smooth μ for those four different geometries. We can clearly conclude that the non–convexity of the obstacle creates local minima for the cost function. More precisely we can see that the reconstruction is poor in the non–convex area of the obstacle.

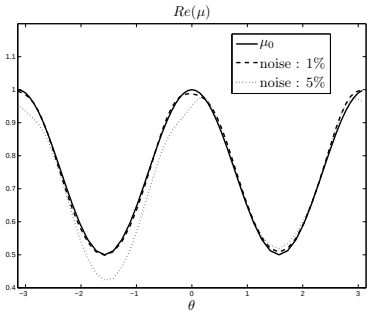

(a) Error(1%) = 2.1%, Error(5%) = 11.2%

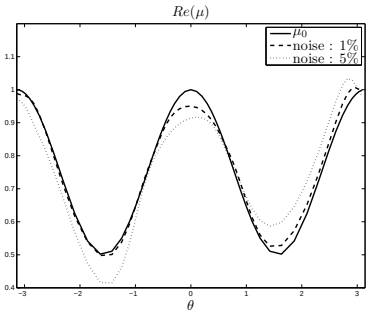

(b) Error(1%) = 3%, Error(5%) = 10.8%

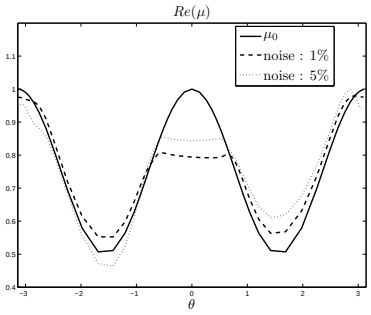

(c) Error(1%) = 3.9%, Error(5%) = 13%

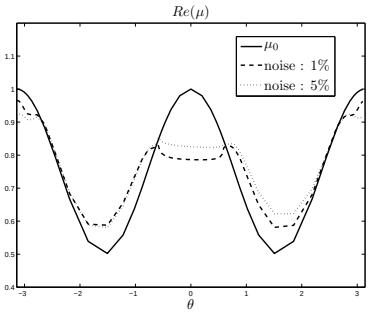

(d) Error(1%) = 9.1%, Error(5%) = 16.2%

Figure 11: *Reconstruction of* $\Re e(\mu_0) = 0.5(1 + cos^2(\theta))$, $\mu_{init} = 0.7$, $\lambda = 0$, *for the four obstacles of Figure 10.*

Simultaneous search for λ and μ. We now study the simultaneous reconstruction of λ and μ on the ellipse (see Figure 4). Table 1 represents the

λ_{obs}	μ_{obs}	λ_{init}	μ_{init}	λ	μ	Error on the far–field
i	1	$0.5i$	0.5	i	0.97	0.05%
i	0.2	$0.5i$	0.1	$0.99i$	0.21	0.08%
i	5	$0.5i$	2.5	$0.97i$	5.12	0.07%

Table 1: *Simultaneous reconstruction of λ and μ constant with the wave number $k = 9$; $\sigma = 1\%$ of noise.*

simultaneous reconstruction of constant λ and μ and we observe a good reconstruction in the constant case. On Figure 4.3.2 we show the reconstruction

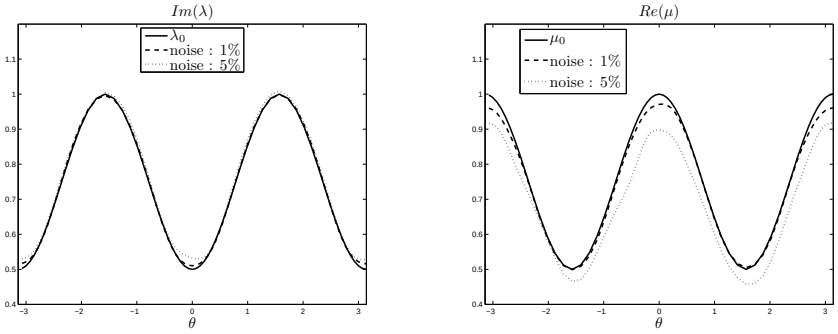

Figure 12: *Wave number $k = 9$, limited aperture data with 10 incident waves, Error (1%) = 2.7%, Error (5%) = 9.8% reconstruction of $\Im m(\lambda_0) = 0.5(1 + sin^2(\theta))$, $\lambda_{init} = 0.7i$ (on the left) and $\Re e(\mu_0) = 0.5(1 + cos^2(\theta))$, $\mu_{init} = 0.7$ (on the right).*

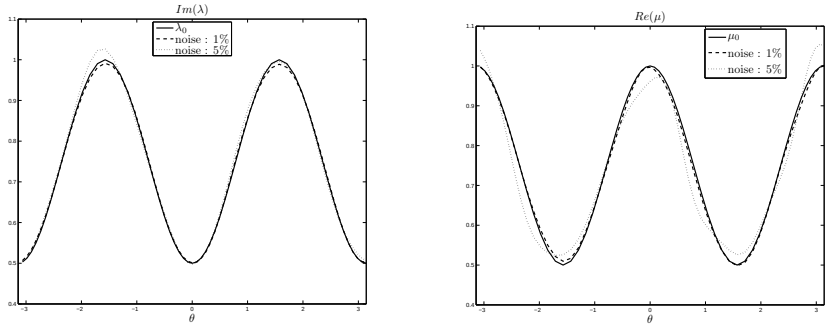

Figure 13: *Wave number $k = 9$, full aperture data with 10 incident waves, reconstruction of $\Im m(\lambda_0) = 0.5(1 + sin^2(\theta))$, $\lambda_{init} = 0.7i$ (on the left) and $\Re e(\mu_0) = 0.5(1 + cos^2(\theta))$, $\mu_{init} = 0.7$ (on the right).*

of functional impedance coefficients λ and μ using $N = 10$ incident waves with aperture equal to $\pi/5$. The reconstruction is quite good for 1% of noise and remains acceptable for 5% of noise.

On Figure 4.3.2 we tried to improve these results by observing everywhere but we still poorly reconstruct μ with a high level of noise. Here, we should note that the reconstruction of the coefficient μ is a much harder task than the reconstruction of λ.

Stability with respect to a perturbed geometry. To illustrate the stability result with respect to the obstacle stated in Theorem 3.6 we construct numerically $u^\infty_{obs}(\cdot, d_i) = T(\lambda_0, \mu_0, \partial D, d_i)$ for a given obstacle D (left hand side of Figure 14) and we minimize the "perturbed" cost function

$$F_\varepsilon(\lambda, \mu) = \frac{1}{2}\sum_{i=0}^{N} \|T(\lambda, \mu, \partial D_\varepsilon, d_i) - u^\infty_{obs}(\cdot, d_i)\|^2_{L^2(S_i)}$$

for a perturbation D_ε (right hand side of Figure 14). The perturbation of the obstacle is denoted γ and defined by

$$\gamma := \frac{\varepsilon_0}{\mathrm{diam}(D)}.$$

Note that the perturbed obstacle is the convex hull of the non–convex obstacle

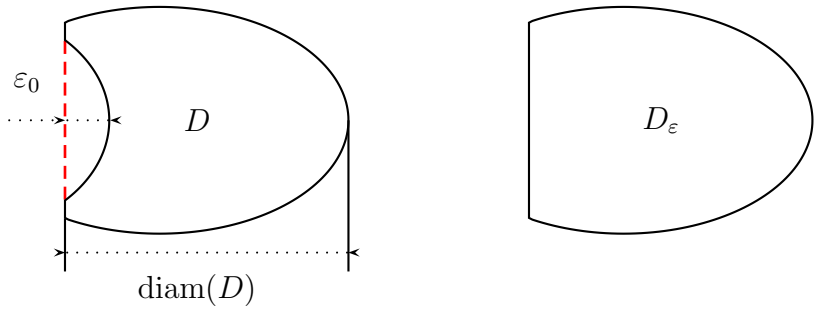

Figure 14: *Exact(left side) and perturbed(right side) geometries.*

D. In the following experiments we want to evaluate the impact of γ on the reconstruction of the coefficients. To satisfy the assumptions of Theorem 3.6 we have to check that we can find some λ_ε and μ_ε such that

$$F_\varepsilon(\lambda_\varepsilon, \mu_\varepsilon) \leq \delta$$

for a small δ. If we take the same uniformly distributed incident directions with $N = 10$ and $k = 9$ as before (the wavelength is more or less equal to the diameter of D), we have

$$\frac{F_\varepsilon(\lambda_0, \mu_0)}{\sum_{i=0}^{N} \|u^\infty_{obs}(\cdot, d_i)\|^2_{L^2(S_i)}} = \begin{cases} 8\% & \text{if } \gamma = 1\% \\ 27\% & \text{if } \gamma = 3\% \end{cases}.$$

These levels of perturbation on the cost function are too high to hope a good reconstruction of the coefficients. It is reasonable to consider we do not enlight the obstacle in the direction of the non–convexity (since we have poor knowledge

of such area). Let us suppose for example that we still have 10 incident waves but now the incident directions belong to $[-\pi/2, \pi/2]$. We have the following relative errors with the actual impedances

$$\frac{F_\varepsilon(\lambda_0, \mu_0)}{\sum_{i=0}^{N} \|u^\infty_{obs}(\cdot, d_i)\|^2_{L^2(S_i)}} = \begin{cases} 3\% & \text{if } \gamma = 1\% \\ 9\% & \text{if } \gamma = 3\% \end{cases} .$$

In this case we hope a good reconstruction of the impedance coefficients at least in the directions of incidence. On Figure 4.3.2 we can see that this is the case for $\gamma = 1\%$ even if we put $\sigma = 5\%$ of noise on the measurements. If we have $\gamma = 3\%$ the reconstruction remains quite good in the non–perturbed area and acceptable in the perturbed area.

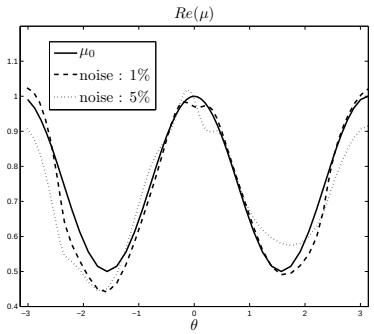

(a) Error (1%) = 2.9%, Error (5%) = 11%

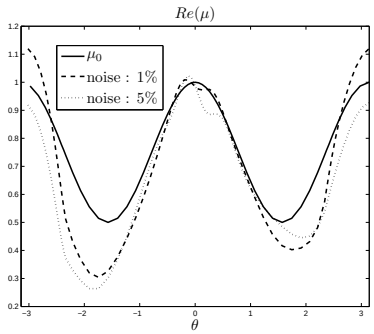

(b) Error (1%) = 8%, Error (5%) = 10.8%

Figure 15: *Perturbed obstacle (see Figure 14), wave number* $k = 9$, $\mu_{init} = 0.7$, $\lambda = 0$, $\gamma = 1\%$ *on the left and* 3% *on the right .*

Acknowledgement

The grant of Nicolas Chaulet is supported by a DGA grant.

References

[1] Grégoire Allaire. *Conception optimale de strctures*. Springer-Verlag, 2007.

[2] A. Bendali and K. Lemrabet. The effect of thin coating on the scattering of time–harmonic wave for the helmholtz equation. *SIAM J. Appl. Math.*, 1996.

[3] Laurent Bourgeois and Houssem Haddar. Identification of generalized boundary conditions in inverse scattering problems. *Inverse Problems and Imaging*, 4(1):19–38, 2010.

[4] Fioralba Cakoni and David Colton. *Qualitative Methods in Inverse Scattering Theory*. Springer-Verlag, 2006.

[5] Fioralba Cakoni, David Colton, and Peter Monk. The determination of the surface conductivity of a partially coated dielectric. *SIAM J. Appl. Math.*, 65(3):767–789, 2005.

[6] Fioralba Cakoni, David Colton, and Peter Monk. The determination of boundary coefficients from far field measurements. *Journal of integral equations and applications*, 22(2), 2010.

[7] David Colton and Rainer Kress. *Inverse acoustic and electromagnetic scattering theory*, volume 93 of *Applied Mathematical Sciences*. Springer-Verlag, second edition, 1998.

[8] Marc Duruflé, Houssem Haddar, and Patrick Joly. Higher order generalized impedance boundary conditions in electromagnetic scattering problems. *C.R. Physique*, 7(5):533–542, 2006.

[9] Houssem Haddar and Patrick Joly. Stability of thin layer approximation of electromagnetic waves scattering by linear and nonlinear coatings. *J. Comput. Appl. Math.*, 2002.

[10] Houssem Haddar, Patrick Joly, and H.-M. Nguyen. Generalized impedance boundary conditions for scattering by strongly absorbing obstacles: The scalar case. *Math. Models Methods Appl. Sci.*, 2005.

[11] Antoine Henrot and Michel Pierre. *Variation et optimisation de formes*, volume 48 of *Mathématiques & Applications*. Springer-Verlag, 2005.

[12] Andreas Kirsch and Natalia Grinberg. *The factorization method for inverse problems*. Oxford University Press, 2008.

[13] Rainer Kress. *Linear integral equations*, volume 82 of *Applied Mathematical Sciences*. Springer-Verlag, 1989.

[14] Christophe Labreuche. Stability of the recovery of surface impedances in inverse scattering. *J. Math. Anal. Appl.*, (231):161–176, 1999.

[15] J. J. Liu, G. Nakamura, and M. Sini. Reconstruction of the shape and surface impedance from acoustic scattering data for an arbitrary cylinder. *SIAM J. Appl. Math.*, 67(4):1124–1146, 2007.

[16] Jean-Claude Nédélec. *Acoustic and Electromagnetic Equations*. Springer-Verlag, 2001.

[17] Pedro Serranho. A hybrid method for inverse scattering for shape and impedance. *Inverse Problems*, 22:663–680, 2006.

[18] E. Sincich. Stable determination of the surface impedance of an obstacle by far field measurements. *SIAM J. Appl. Math.*, 38(2):434–451, 2006.

[19] Mourad Sini, Lin He, and Stefan Kindermann. Reconstruction of shapes and impedance functions using few far–fields measurements. *Journal of computational physics*, 2009.

[20] Mourad Sini and G. Nakamura. Obstacle and boundary determination from scattering data. *SIAM J. Appl. Math.*, 2007.

[21] www.freefem.org/ff++. *FreeFem++*.

Centre de recherche INRIA Saclay – Île-de-France
Parc Orsay Université - ZAC des Vignes
4, rue Jacques Monod - 91893 Orsay Cedex (France)

Centre de recherche INRIA Bordeaux – Sud Ouest : Domaine Universitaire - 351, cours de la Libération - 33405 Talence Cedex
Centre de recherche INRIA Grenoble – Rhône-Alpes : 655, avenue de l'Europe - 38334 Montbonnot Saint-Ismier
Centre de recherche INRIA Lille – Nord Europe : Parc Scientifique de la Haute Borne - 40, avenue Halley - 59650 Villeneuve d'Ascq
Centre de recherche INRIA Nancy – Grand Est : LORIA, Technopôle de Nancy-Brabois - Campus scientifique
615, rue du Jardin Botanique - BP 101 - 54602 Villers-lès-Nancy Cedex
Centre de recherche INRIA Paris – Rocquencourt : Domaine de Voluceau - Rocquencourt - BP 105 - 78153 Le Chesnay Cedex
Centre de recherche INRIA Rennes – Bretagne Atlantique : IRISA, Campus universitaire de Beaulieu - 35042 Rennes Cedex
Centre de recherche INRIA Sophia Antipolis – Méditerranée : 2004, route des Lucioles - BP 93 - 06902 Sophia Antipolis Cedex

Éditeur
INRIA - Domaine de Voluceau - Rocquencourt, BP 105 - 78153 Le Chesnay Cedex (France)
http://www.inria.fr
ISSN 0249-6399